Desalination and Water Treatment
www.deswater.com
doi: 10.1080/19443994.2015.1088474

57 (2016) 18157–18167
August

Taylor & Francis
Taylor & Francis Group

Evaluation on the efficiency of ethylenediaminetetraacetic acid (EDTA)-modified rice husk as a low-cost sorbent for various dyes removal under continuous flow condition

Siew-Teng Ong[a,b,*], Weng-Nam Lee[c,1]

[a]*Faculty of Science, Universiti Tunku Abdul Rahman, Jalan Universiti, Bandar Barat, Kampar, Perak 31900, Malaysia, Tel. +60 5 4688888; Fax: +60 5 4661676; emails: ongst@utar.edu.my, ongst_utar@yahoo.com*
[b]*Centre for Biodiversity Research, Universiti Tunku Abdul Rahman, Jalan Universiti, Bandar Barat, Kampar, Perak 31900, Malaysia*
[c]*Faculty of Engineering and Science, Department of Science, Universiti Tunku Abdul Rahman, Jalan Genting Kelang, Setapak, Kuala Lumpur 53300, Malaysia, email: elvislee_1122@yahoo.com*

Received 26 January 2015; Accepted 24 August 2015

ABSTRACT

The potential of ethylenediaminetetraacetic acid (EDTA)-modified rice husk (ERH) as a sorbent to remove both methylene blue (MB) and reactive orange 16 (RO 16) in single and binary dye solutions was studied. Surface characterization of natural rice husk and ERH was investigated using field emission scanning electron microscope (FESEM) and atomic force microscope (AFM). From the FESEM micrographs, due to the absence of pores and cavities, it can be concluded that ERH is a non-porous material. The adsorption behaviour of MB and RO 16 onto column packed with ERH was investigated under continuous flow mode with three different parameters: the effect of influent concentration, the effect of bed depth and the effect of flow rate. Column studies indicated that the breakthrough time is longer for MB at lower influent concentration and flow rate. Unusual breakthrough curves were obtained for RO 16 in both single and binary dye solutions with very rapid initial breakthrough. This implies that the adsorption of RO 16 is a slow process and an effective adsorption only takes place after a sufficient lapse of time. Different mathematical models were used to characterize the fixed-bed performance for the adsorption process involved, namely bed depth service time (BDST) model, Adams–Bohart model and Clark model.

Keywords: EDTA modified rice husk; Adsorption; Methylene blue; Reactive orange 16; Breakthrough curve; Adams–Bohart; Clark model

1. Introduction

The usage of synthetic dyes in many industries such as textile, paper, plastics and cosmetics has experienced phenomenal growth in the past several decades. This subsequently led to a dramatic increase in dye waste volume. Presently, there are more than 100,000 commercial dyes with a rough estimated production of 7×10^5 tons per year [1–3]. However,

*Corresponding author.

[1]Current address: Heriot Watt University, Malaysia Campus, No. 1 Jalan Venna P5/2, Precinct 5, 62200 Putrajaya.

dye wastewater poses a serious threat to the environment due to its toxicity and appearance [4]. Majority of dyes are visually detected even at the concentration of less than 1 mg/L. Based on the dissociation of dyes in water, it can be classified into three categories, namely acidic, basic and disperse dyes. The complicated molecular structures of dyes make dyes wastewater difficult to be treated using conventional biological and physicochemical processes.

Adsorption of dye effluents onto activated carbon has been considered as the most efficient method for the removal of various dyes. However, the high production and regeneration cost are the main reasons that retard the application of activated carbon for dyes removal on a wide scale [5]. Hence, attempts have been made by many researchers to prepare an alternative low-cost sorbents. Utilization of agricultural waste such as peanut hull, tea waste, paddy straw, coffee waste, pomelo peel, baggage pith and hen feather as low-cost sorbent is of great interest as these materials are available at almost free of cost [6–10].

However, in most of the studies, attention has been focused on batch experiments whereby the adsorption process is confined to the treatment of small volumes of effluent under equilibrium conditions. The information gathered from batch type processes does not give accurate scale-up data under continuous flow conditions and most importantly, the effects of adsorbent recycling and regeneration cannot be studied. Therefore, it is crucial to carry out flow tests using columns since this method has closer simulation to the commercial systems. The results gathered from the column study are useful to obtain design models which would be applicable to commercial systems.

Rice husk is generated as a waste during the first stage of rice milling, when rough rice or paddy rice is husked (husk is separated from the rest of the grain). Generally, the husk represents on average about 20% of the rough harvested weight of rice. In rice producing countries like Malaysia, more than 350,000 metric tonnes of rice husks are produced annually from paddy cultivation [11]. Therefore, the utilization of this abundant agricultural waste is of great significance. The high silica content in rice husk can provide good mechanical strength without any additional cross-linking process that will add on to the cost of production. It is expected that chemical modification would further enhance their usefulness in the treatment of wastewater.

The ultimate usefulness of the modified material is its capability in removing different types of dyes such as basic and reactive dyes as these do commonly occur together in industrial effluents. The suitability of the modified rice husk was being assessed under continuous flow condition as this resembles the actual practice in wastewater treatment. Characterization analysis by Fourier-transform infrared spectrophotometer (FTIR), field emission scanning electron microscope (FESEM) and atomic force microscope (AFM) were also performed. The results obtained from both batch and column studies showed that under controlled laboratory conditions, an appreciable amount of both dyes could be removed by ERH. Therefore, the investigated adsorbent could be used as a low-cost adsorbent to remove dyes from textile wastewater.

2. Materials and methods

2.1. Sorbent

The rice husk was collected from a local rice mill. It was washed thoroughly with water to ensure the removal of dust and ash. Rice husk was then rinsed several times with distilled water and dried overnight in an oven at 50°C. The dried rice husk was then ground to pass through a 1-mm sieve and labelled as natural rice hull (NRH). The modification with ethylenediaminetetraacetic acid (EDTA) was carried out by varying temperature and the ratio of EDTA to rice husk. Based on the uptake results, the optimum condition for the modification of rice husk were by treating 8 g of grinded rice husk with 0.5 g of EDTA and soaked in 300 mL of 1.0 M sodium hydroxide (NaOH) for 3 h at 70°C. The treated rice husk was filtered and washed with excess water until neutral before subjected to drying process at 60°C. The dried material was labelled as ERH.

2.2. Sorbates

Methylene blue (MB) and RO 16 were the sorbates used in this study. The cationic dye MB (C.I. = 52,015, 95% dye content) and anionic dye RO 16 (C.I. = 17,757, 50% dye content) were used without further purification. All dye powders used in this study were purchased from Sigma-Aldrich Pte. Ltd (United States of America). The structures of dyes are shown in Fig. 1. A stock solution of 1,000 mg/L was prepared for both MB and RO 16 and subsequently diluted when necessary for further analysis. The binary dye solution was obtained through the mixing of both dyes.

2.3. Instrumental and characterization analysis

The functional groups of NRH and ERH were determined using FTIR spectrophotometer at the wavenumber range of 400–4,000 cm^{-1}. The surface morphology of the sorbents was studied using field

Methylene Blue (MB)

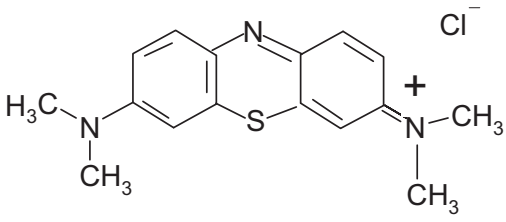

Reactive Orange 16 (RO16)

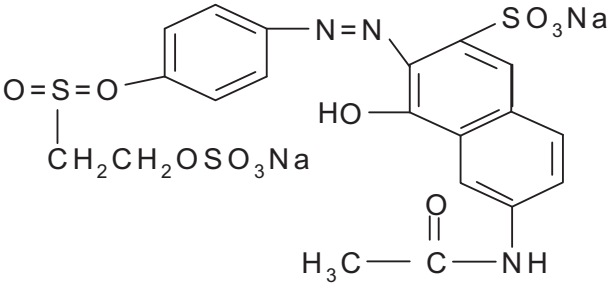

Fig. 1. Dye structure of MB and RO16.

emission scanning electron microscope (FESEM) which is operated at emission current of 3.0 kV with working distance of 4.6 mm-JEOL FESEM JSM 6701F. As for surface topography, it was examined through atomic force microscope, AFM (Quensant Q-Scope 250).

2.4. Column study

Column studies were conducted using a glass column of 1.0-cm internal diameter. Cotton wool was placed at the bottom of the column covered with a layer of washed sand to prevent leakage of the sorbent. Distilled water was run through the column prior to the dye solutions to achieve hydraulic equilibrium. The column was then fed with dye solution and the eluants were collected at 10-ml fractions. A peristaltic pump was used to control the flow rate of eluant. The eluant was analysed for its dyes concentration using single-beam UV–vis spectrophotometer with the maximum absorption wavelength of 664 and 494 nm for MB and RO 16, respectively.

2.4.1. Effect of influent concentration

The effect of different influent concentrations of dye solution on the breakthrough curve was studied using 5, 10 and 15 mg/L for MB and RO 16 in both single and binary dye solutions. The column was packed to a height of 7.0 cm using 1.0 g of ERH. The flow rate was maintained at 10 mL/min.

2.4.2. Effect of bed depth

As for the effect of bed depth, the column was packed with 0.5, 0.75 and 1.0 g of ERH to a height of 2.5, 4.5 and 7.0 cm, respectively. The flow rate was maintained at 10 mL/min and the influent concentration of dye was fixed at 10 mg/L.

2.4.3. Effect of flow rate

The flow rate was varied from 5 to 15 mL/min. The bed depth and influent concentration were fixed at 7 cm in height and 10 mg/L, respectively.

3. Results and discussion

3.1. Instrumental analysis

3.1.1. Fourier transform infrared spectroscopy (FTIR)

Fig. 2 shows the FTIR spectra of both NRH and ERH. Absorption peaks at 3,413 and 3,432 cm^{-1} for both NRH and ERH, respectively, are due to the O–H stretching vibrations. The wide O–H peak observed in both NRH and ERH are due to the vibrational mode that being complicated by hydrogen bonding. The modification of NRH by EDTA will yield carboxyl groups and quaternary amine groups on the surface of NRH. Therefore, ERH spectrum showed a peak at 1,637 cm^{-1} which indicates the presence of C=O stretch or conjugated C=C. The same peak was observed in the spectrum of NRH. This might be due to the presence of lignin in rice husk which consists of both carbonyl group and C=C stretch. No N–H stretch was observed in the spectrum of ERH near region 3,310–3,500 cm^{-1} as the amine groups present are in quaternary structure. Another broad peak was observed in the spectrum of NRH at 1,096 cm^{-1} which could be indicative of C–O anti-symmetrical stretching. This C–O stretching was absent in the spectrum of ERH because the OH groups of NRH were being substituted by EDTA during the modification process. The peaks at 467 to 800 cm^{-1} in the spectrum of NRH are attributed to the Si–H groups indicating the presence of silica. From the ERH spectrum, these peaks were not observed. This is due the modification process that might reduce the percentage of silica in ERH.

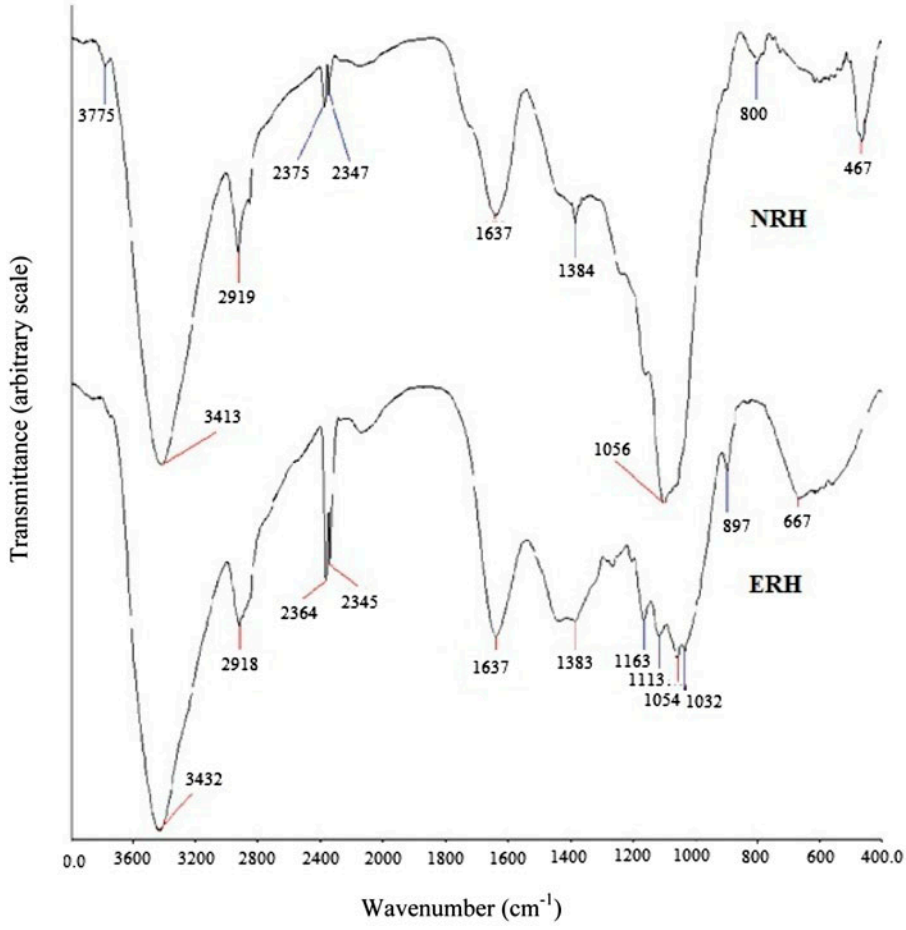

Fig. 2. Infrared spectra of NRH and ERH.

3.1.2. Surface characterizations

The FESEM micrographs of NRH and ERH are shown in Figs. 3 and 4, respectively. It was noticed that the surface texture of ERH appeared to be smoother as compared to NRH which showed a rough and heterogeneous surface. This is due to the introduction of both amine and carboxyl groups on the surface of rice husk using EDTA. It was also found that both NRH and ERH are non-porous materials due to the absence of cavities and pores.

The surface topography of NRH and ERH was studied using contact mode by AFM on a $20 \times 20\ \mu m^2$ area as shown in Figs. 5 and 6, respectively. Colour mapping was used to display the data where light colour indicates high topography, whereas darker colour shows lower topography. With the addition of carboxyl and amine groups, surface of rice husk becomes more intense. Hence, a higher topography (lighter colour) was observed for ERH.

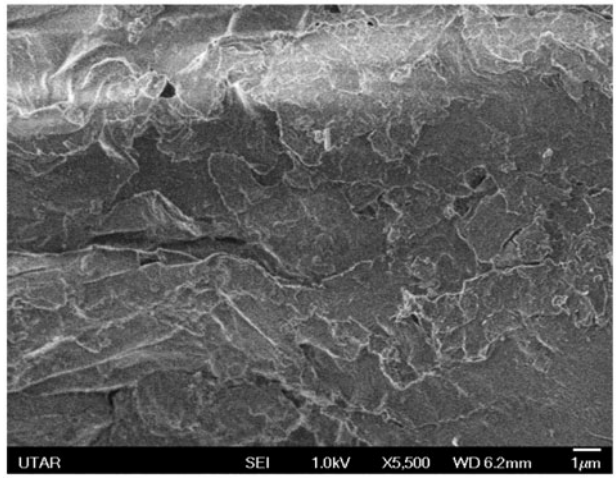

Fig. 3. SEM micrograph of NRH.

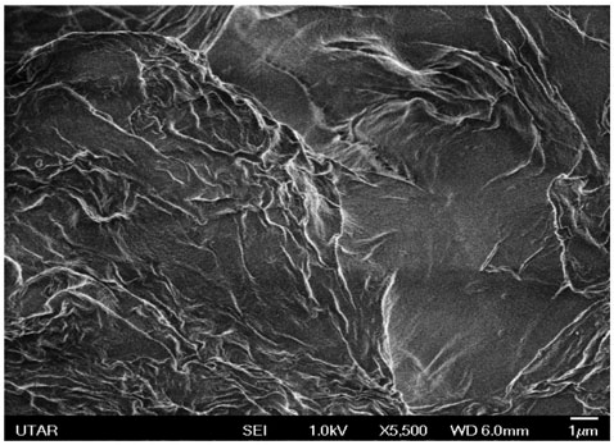

Fig. 4. SEM micrograph of ERH.

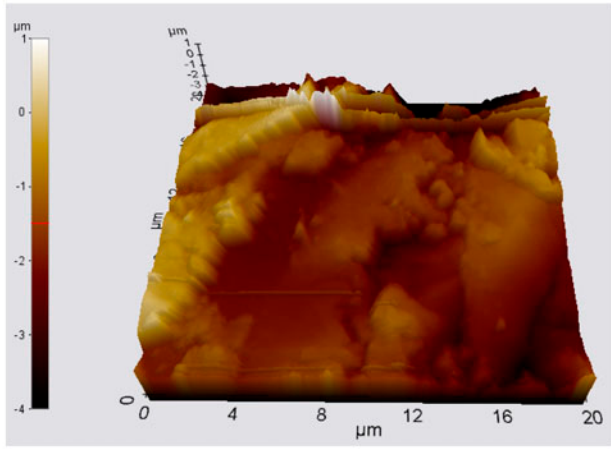

Fig. 5. AFM topography picture of NRH.

3.1.3. Adsorption mechanism

In this study, when rice husk was modified with EDTA, the proposed reaction shown below is postulated to take place:

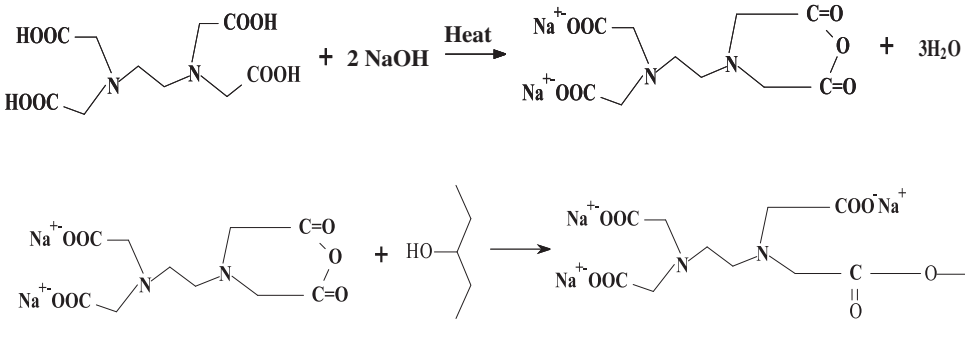

(1)

where

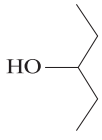

represents the surface of natural rice husk (NRH).

The presence of hydroxyl group played an important role in the EDTA modification process. EDTA was heated to form anhydride by removing water molecule from two carboxyl groups. The anhydride formed will react with the hydroxyl group of rice husk forming ester [12]. The EDTA-modified rice husk (ERH) contains two positively charge quaternary amine groups and four negatively charged carboxyl groups when immersed in water. The positively charged amine groups attract the negatively charged sulphonate groups present in RO 16 dye molecule, whereas the negatively charged carboxyl groups are likely to be responsible for the adsorption of positively charged MB molecule. The adsorption of both MB and RO 16 dye molecule is proposed as below:

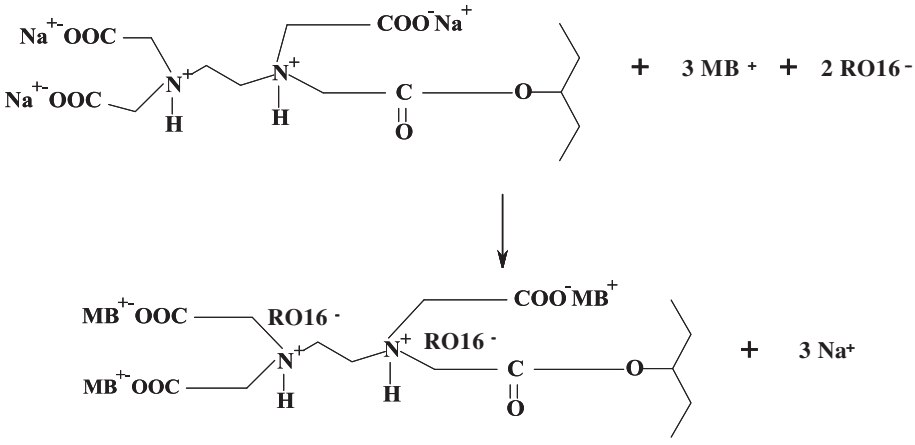

(2)

As for the adsorption of dyes in binary dye solutions, the percentage uptake of RO 16 was enhanced as compared to single dye solution and this could be related to the surface charge of ERH upon the adsorption of MB molecules. The reaction is postulated as follows:

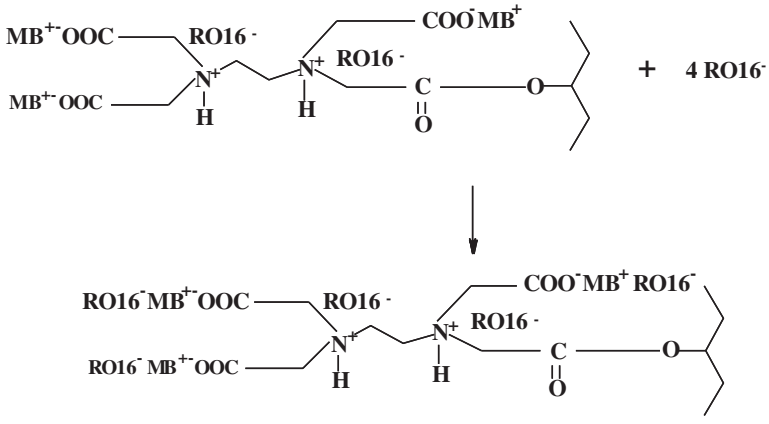

(3)

For the synergistic effect observed in binary dye solution, it can be closely related to the adsorption of MB dye molecules. The adsorbed MB molecules increase the positive charges on the surface of ERH and subsequently enhance the adsorption of RO 16.

3.2. Column study

3.2.1. Effect of influent concentration

The uptake of MB and RO 16 was studied at different influent concentrations ranging from 5 to 15 mg/L with other variables being held constant. The breakthrough curves of MB in single dye solution are shown in Fig. 7. A steeper "S"-shaped curve was obtained at higher influent concentration with lower breakthrough volume. The breakthrough was observed at 870, 480 and 430 mL of dye solutions for influent concentration of 5, 10 and 15 mg/L, respectively. The data showed that the breakthrough time for single MB increased with decreasing influent concentration. This is because at a lower influent concentration, a weaker driving force would be anticipated due to the lower mass transfer from the bulk solution to the particle surface. As such, a longer time is needed for the binding sites to become saturated. Similar trend was observed for binary MB breakthrough curves. Sivakumar and Palanisamy [4] also reported that with an increasing initial dye concentration of acid blue 92 and basic red 29, the breakthrough curves become steeper and the breakthrough volume decreases.

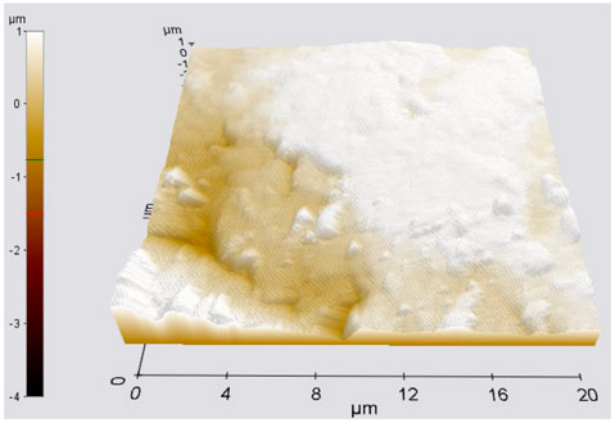

Fig. 6. AFM topography picture of ERH.

In the case of RO 16, a rapid initial breakthrough was apparent in both binary and single dye solutions before effective adsorption could take place (Fig. 7). This indicates that binding of RO 16 on ERH, though efficient, was a slow process. The rapid breakthrough could be due to the insufficient time for the sorbent to be protonated as it has been proposed that the sorption of anions occurs through electrostatic interactions. As the sorbent in the unprotonated state was unable to retain the solute, initial breakthrough occurred. Sufficient lapse of time was required before the dye molecules could be sorbed onto the column. This result was similar to the previously reported work by Lee et al. [13]. The enhancement shown in the adsorption of RO 16 in binary dye solutions is most probably due to the surface charge of ERH upon adsorption of MB.

3.2.2. Adams–Bohart model

Adams–Bohart model is a model used to determine the mass transfer coefficient of an adsorption process in a continuous mode condition. The linearized Adams–Bohart equation is as follows [14]:

$$\ln\frac{C_t}{C_0} = K_{AB}C_0 t - K_{AB}q_{AB}\frac{H}{v} \tag{4}$$

where C_t is the eluant concentration at time t (mg/L), C_0 is the influent concentration (mg/L), K_{AB} is the mass transfer coefficient (L/min mg), q_{AB} is the amount of dye solution untaken by adsorbent (mg/L), v is the linear flow rate of solution (mL/min), H is the bed height (m) and t is the time (min).

From the Adams–Bohart modelling, the mass transfer coefficient K_{AB} is a diffusion rate constant that relates to mass transfer area and mass transfer rate. This constant value can be determined from the slope of the Adams–Bohart plot (Fig. 8), which can be used to quantify the mass transfer between a fluid and a solid. As recorded in Table 1, the mass transfer coefficient decreases with an increasing influent concentration of MB in single and binary dye solutions. This indicates that the mass transfer of the dye molecules from the bulk solution to the surface of ERH is more favourable at lower concentration [15]. As for the R^2 value, it shows that the experimental data fitted reasonably well in Adams–Bohart model.

The applicability of Adams–Bohart model requires the experimental data to exhibit a typical "S" shape. However, for RO 16, it is apparent that it demonstrated a packed bed sorption pattern which does not follow an "S" shape and therefore this model is not applicable.

3.2.3 Effect of bed depth

The effect of bed depth in the uptake of single MB dye solution shows that higher bed depth causes

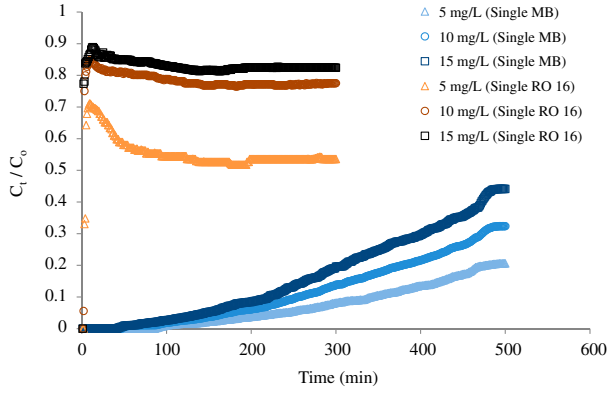

Fig. 7. Effect of influent concentrations on the breakthrough curves of single MB and RO 16 dye solution.

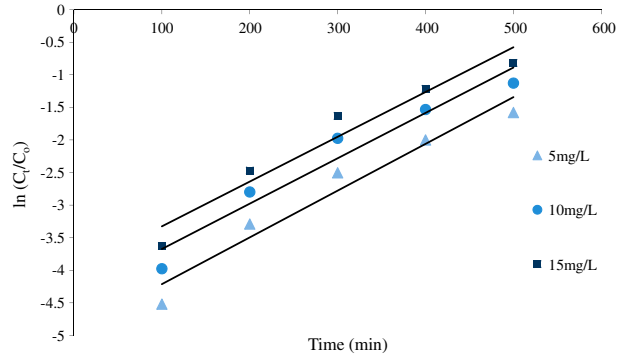

Fig. 8. Adams–Bohart plot for the removal of MB single at different influent concentrations.

Table 1
Adams–Bohart constants

Dyes	Influent concentration (mg/L)	Bed depth (cm)	Flow rate (mL/min)	k (mass transfer coefficient)	R^2
MB single	5.0	7.0	10.0	0.00140	0.950
	10.0	7.0	10.0	0.00070	0.945
	15.0	7.0	10.0	0.00040	0.943
	10.0	2.5	10.0	0.00038	0.815
	10.0	4.5	10.0	0.00040	0.815
	10.0	7.0	10.0	0.00071	0.944
	10.0	7.0	5.0	0.00196	0.878
	10.0	7.0	10.0	0.00043	0.998
	10.0	7.0	15.0	0.00028	0.863
MB binary	5.0	7.0	10.0	0.00108	0.997
	10.0	7.0	10.0	0.00060	0.984
	15.0	7.0	10.0	0.00041	0.979
	10.0	2.5	10.0	0.00038	0.815
	10.0	4.5	10.0	0.00040	0.815
	10.0	7.0	10.0	0.00080	0.939
	10.0	7.0	5.0	0.00192	0.861
	10.0	7.0	10.0	0.00055	0.959
	10.0	7.0	15.0	0.00028	0.852

longer breakthrough time (Fig. 9). It was found that at 50% breakthrough curve, the breakthrough time ($t_{0.5}$) increased from 192 min to 201 and to 335 min for bed depth of 2.5, 4.5 and 7.0 cm, respectively. The higher the bed depth, the longer the service time before breakthrough occurred. This was attributed to the increase in binding sites on the adsorbent and thus a longer time was required for the column to become saturated since feed dye concentration and flow rate were constant. The results showed that by varying the bed depth from 4.5 to 7.0 cm, it has little effect on the breakthrough curves of MB. This is due to the rapid adsorption of MB by ERH. Based on the mass transfer coefficient value calculated from the slope of the Adams–Bohart plot (Table 1), at lower bed depth, the mass transfer rate between MB molecules and ERH is also lower. The breakthrough curve data fitted well in Adams–Bohart model ($R^2 = 0.944$) when the column height was fixed at 7 cm. Similar findings were obtained for MB in binary dye solution (Fig. 10). As shown in Table 1, it can be seen that the mass transfer coefficient value increased with an increasing bed depth, indicating higher mass transfer rate of MB molecules onto ERH.

Similar results were obtained in the study whereby a packed column of *Euphorbia antiquorum* L activated carbon was used for the uptake of acid blue 92 and basic red 29. The authors reported that the throughput volume of dye solution increases with an increase in bed depth due to the availability of more adsorption sites [4].

Figs. 9 and 10 showed the breakthrough curves for RO 16 in both single and binary dye solutions. With the same concentrations of 10 mg/L and at the constant flow rate of 10 mL/min, breakthrough occurred almost immediately at the beginning of the column operation (at the first 100 mL of feed volume). The adsorption behaviour of RO 16 demonstrated the same trend: an immeasurably fast breakthrough followed by an effective adsorption. This is most probably due to the insufficient time for the protonation of ERH to be

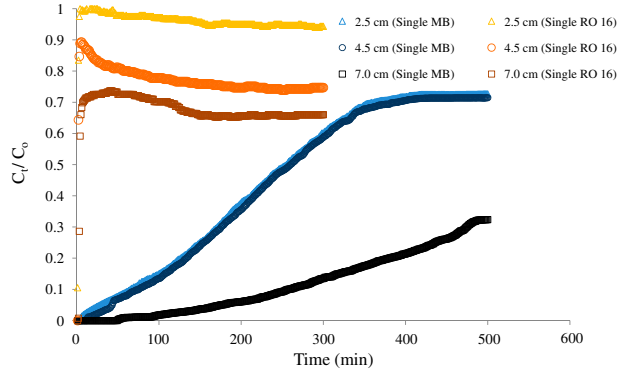

Fig. 9. Effect of bed depth on the breakthrough curves of single MB and RO 16 dye solution.

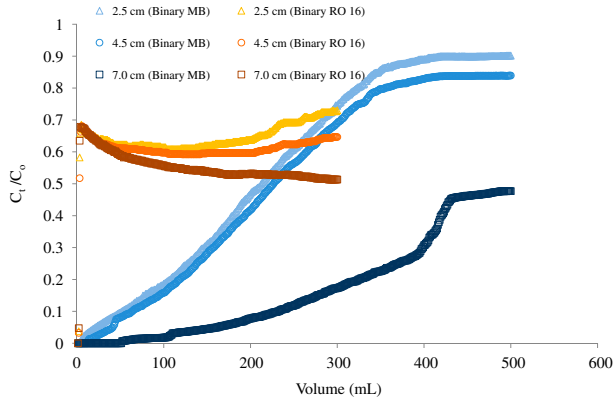

Fig. 10. Effect of bed depth on the breakthrough curves of binary MB and RO 16 dye solution.

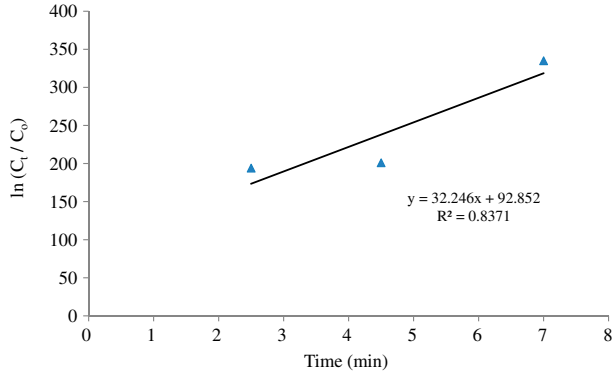

Fig. 11. BDST plot for MB single dye solution.

occurred as suggested earlier. Generally, the percentage of dye removal increased with an increasing bed depth. The adsorption data for single RO 16 showed that at 3,000 mL of eluant volume, the values of C_t/C_0 decreased from 0.94 to 0.66 as the column height increased from 2.5 to 7.0 cm. This suggests that with the introduction of more adsorption sites, a better adsorption can be achieved. Besides, the adsorption of RO 16 in binary dye solutions was enhanced as compared to single dye solutions and this could be related to the surface charge of the ERH upon adsorption of MB molecules.

3.2.4 BDST model

The bed depth service time (BDST) model is commonly used to measure the capacity of a specific bed depth at different breakthrough values. BDST model assumed that both intraparticle mass transfer resistance and external film resistance are negligible. These assumptions enable the model to provide useful modelling equations for the changes in the system parameters [16]. The equation of BDST model is as follows [14]:

$$t = \frac{N_0}{C_0 F} Z - \frac{1}{K_a C_0} \ln\left(\frac{C_0}{C_t} - 1\right) \quad (5)$$

where C_t = eluant concentration at time t (mg/L), C_0 = influent concentration (mg/L), F = influent linear velocity (cm/min), N_0 = adsorption capacity (mg/g), K_a = rate constant (L/mg min), t = time (min), and Z = bed depth of column (cm).

The linear curve of BDST model at 50% breakthrough for single MB is shown in Fig. 11. According to BDST model (Eq. (2)), a straight line that passing through the origin should be obtained. However, the results showed a straight line which does not pass through the origin with low R^2 value was obtained. This indicates that the adsorption of MB onto the column in single and binary dye solutions may consist of more than one rate-controlling step [13,17]. The experimental data of RO 16 in both single and binary dye solutions were not tested on BDST model as the breakthrough curves did not exhibit the typical "S" shape of the packed bed adsorption system which is a prerequisite for BDST model.

3.2.5 Effect of flow rate

Fig. 12 shows the breakthrough curves of MB in single dye solutions at different flow rates from 5 to 15 mL/min. The typical "S"-shaped curves were obtained for MB in single dye solution. The results showed that the breakthrough time appeared to be shorter, from 2,980 mL decreased to 450 mL as the

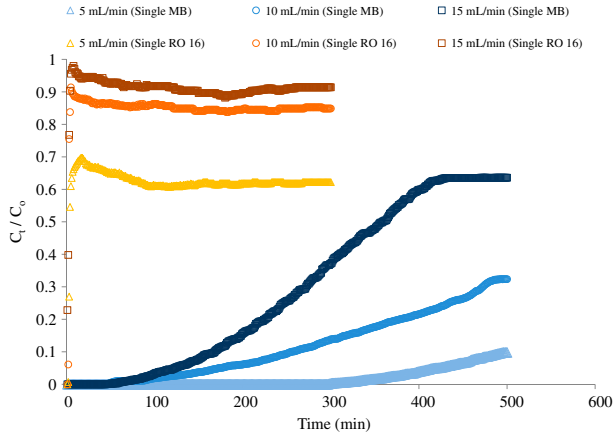

Fig. 12. Effect of flow rate on the breakthrough curves of single MB and RO 16 dye solution.

flow rate increased from 5 to 15 mL/min. This is attributed to the decrease in contact time between ERH and dye molecules and hence the dye molecules leave the column before efficient adsorption could take place. This phenomenon is in agreement with the observed trend whereby the mass transfer coefficient decreases with increasing flow rate as shown in Table 1.

The beneficial effect of reducing the flow rate is that it will prolong the contact time between the adsorbent and adsorbate and therefore leading to a greater volume of the adsorbate solutions to be treated. For RO 16, due to the slow interaction between ERH and the dye molecules, it was found that the values of C_t/C_0 increased with an increasing flow rate, indicating less adsorption occurred at higher flow rate. This is because the dye molecules have less time to penetrate and diffuse into the centre of adsorbent and consequently left the column before efficient adsorption takes place. With the introduction of lower flow rate, this prolongs the contact time between the sorbent and sorbate and subsequently more sorbate can be retained on the column. Since the efficiency of the column depends on the flow rate, it is important to have an appropriate flow rate to make the process more time efficient.

3.2.6 Clark model

Clark model is a mathematical model that incorporates Freundlich equation [18]. As such, this model could be a suitable model for modelling the experimental data as the previous finding showed that the adsorption of MB and RO 16 onto ERH in single and binary dye solutions fitted well in Freundlich isotherm. The equation involved is as follows:

$$\frac{C_t}{C_0} = \left(\frac{1}{1 + Ae^{-rt}}\right)^{1/n-1} \tag{6}$$

where C_t = eluant concentration at time t (mg/L), C_0 = influent concentration (mg/L), A = Clark equation constant, r = Clark equation constant (1/min) and n = Freundlich constant.

The experimental data for the effect of flow rate were modelled using Clark model and the predicted breakthrough curve showed a good agreement with the experimental breakthrough curve for the adsorption of MB in both single and binary dye solutions (Fig. 13). For RO 16, as a rapid initial breakthrough was apparent in both single and binary dye solutions; therefore, Clark model was not applied on the data for this dye as it does not match the prerequisite of the model.

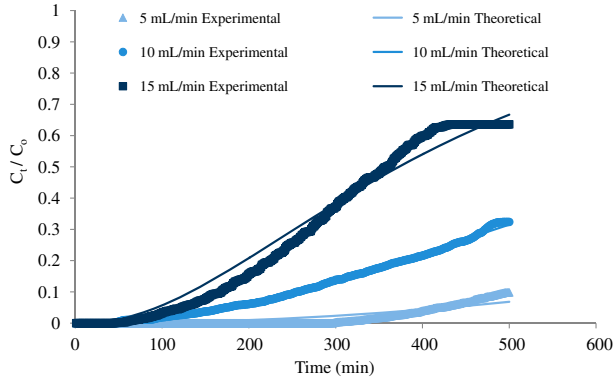

Fig. 13. Comparison between the experimental breakthrough curves and the Clark model predicted breakthrough curves at different flow rates for MB single dye solution.

4. Conclusion

The results obtained from FESEM and AFM analyses showed that the surface texture of ERH is smoother and much more intense as compared to NRH. The experimental data indicated that the adsorption process of both dyes onto ERH was more favourable at lower influent concentration, higher bed depth and lower flow rate. The adsorption of MB onto ERH in both single and binary dye solutions followed the typical "S"-shaped curve under continuous flow mode. However, the adsorption of RO 16 in both single and binary dye solutions showed a rapid breakthrough in the first 5 min followed by a gradual adsorption. By comparing the breakthrough curves for both dyes, it was found that the adsorption process seems to be more efficient in binary dye solution as compared to single dye system. This might be due to the synergistic effect between the adsorbed dyes and the dye molecules from the bulk solution. The predicted breakthrough curves from Clark model agreed well with the experimental breakthrough curves at various flow rates. Mass transfer coefficient obtained from Adams–Bohart model showed a greater adsorption capacity of MB and RO 16 onto ERH at higher bed depth and lower flow rate.

Acknowledgements

The authors are thankful for the financial support by the International Foundation for Science, Stockholm, Sweden and the Organisation for the Prohibition of Chemical Weapons, The Hague, The Netherlands and research

facilities and teaching assistantship for W.N. Lee by Universiti Tunku Abdul Rahman (UTAR).

References

[1] J.W. Lee, S.P. Choi, R. Thiruvenkatachari, W.G. Shim, H. Moon, Evaluation of the performance of adsorption and coagulation processes for the maximum removal of reactive dyes, Dyes Pigm. 69 (2006) 196–203.
[2] A. Demirbas, Agricultural based activated carbons for the removal of dyes from aqueous solutions: A review, J. Hazard. Mater. 167 (2009) 1–9.
[3] S.T. Ong, S.Y. Tan, E.C. Khoo, S.L. Lee, S.T. Ha, Equilibrium studies for Basic blue 3 adsorption onto durian peel (*Durio zibethinus* Murray), Desalin. Water Treat. 45 (2012) 161–169.
[4] P. Sivakumar, P.N. Palanisamy, Packed bed column stdies for the removal of acid blue 92 and basic red 29 using non-conventional adsorbent, Indian J. Chem. Technol. 16 (2009) 301–307.
[5] Y.S. Al-Degs, M.A.M. Khraisheh, S.J. Allen, M.N. Ahmad, Adsorption characteristics of reactive dyes in columns of activated carbon, J. Hazard. Mater. 165 (2009) 944–949.
[6] B. Ramaraju, P.M.K. Reddy, C. Subrahmanyam, Low cost adsorbents from agricultural waste for removal of dyes, Environ. Prog. Sustainable Energy 33 (2014) 38–46.
[7] M. Foroughi-Dahr, H. Abolghasemi, M. Esmaili, A. Shojamoradi, H. Fatoorehchi, Adsorption characteristics of congo red from aqueous solution onto tea waste, Chem. Eng. Commun. 202 (2015) 181–193.
[8] M.E. Argun, D. Güclü, M. Karatas, Adsorption of Reactive Blue 114 dye by using a new adsorbent: Pomelo peel, J. Ind. Eng. Chem. 20 (2014) 1079–1084.
[9] R. Lafi, A. Ben Fradj, A. Hafiane, B.H. Hameed, Coffee waste as potential adsorbent for the removal of basic dyes from aqueous solution, Korean J. Chem. Eng. 31 (2014) 2198–2206.
[10] A. Mittal, V. Thakur, J. Mittal, H. Vardhan, Process development for the removal of hazardous anionic azo dye congo red from wastewater by using hen feather as potential adsorbent, Desalin. Water Treat. 52 (2014) 227–237.
[11] Annual Report of Bernas Sdn Bhd, 2008. URL: <http://www.bernas.com.my/annual.htm>, (Accessed on 8th June 2009).
[12] K.A.G. Gusmão, L.V.A. Gurgel, T.M.S. Melo, L.F. Gil, Adsorption studies of methylene blue and gentian violet on sugarcane bagasse modified with EDTA dianhydride (EDTAD) in aqueous solutions: Kinetic and equilibrium aspects, J. Environ. Manage. 118 (2013) 135–143.
[13] C.K. Lee, S.T. Ong, Z. Zainal, Ethylenediamine modified rice hull as a sorbent for the removal of Basic Blue 3 and Reactive Orange 16, Int. J. Environ. Pollut. 34 (2008) 246–260.
[14] G.S. Bohart, E.Q. Adams, Some aspects of the behavior of charcoal with respect to chlorine. 1, J. Am. Chem. Soc. 42 (1920) 523–544.
[15] N. Kannan, S. Murugavel, Column studies on the removal of dyes Rhodamine-B, Congo Red, and Acid Violet by adsorption on various adsorbents, EJEAF-Chem. 6 (2007) 1860–1868.
[16] D.C.K. Ko, J.F. Porter, G. McKay, Optimised correlations for the fixed-bed adsorption of metal ions on bone char, Chem. Eng. Sci. 55 (2000) 5819–5829.
[17] K.K. Wong, C.K. Lee, K.S. Low, M.J. Haron, Removal of Cu and Pb from electroplating wastewater using tartaric acid modified rice husk, Process Biochem. 39 (2003) 437–445.
[18] R.M. Clark, Evaluating the cost and performance of field-scale granular activated carbon systems, Environ. Sci. Technol. 21 (1987) 573–580.